IEEE Access
Multidisciplinary | Rapid Review | Open Access Journal

Received April 19, 2017, accepted May 20, 2017, date of publication May 30, 2017, date of current version June 27, 2017.

Digital Object Identifier 10.1109/ACCESS.2017.2709254

Energy-Efficient Vector OFDM PLC Systems With Dynamic Peak-Based Threshold Estimation

AUGUSTINE IKPEHAI[1], (Graduate Student Member, IEEE), BAMIDELE ADEBISI[1], (Senior Member, IEEE), KHALED MAAIUF RABIE[1], (Member, IEEE), MICHAEL FERNANDO[1], and ANDREW WELLS[2], (Member, IEEE)

[1]School of Electrical Engineering, Manchester Metropolitan University, Manchester M1 5GD, U.K.
[2]Jaguar Land Rover Limited, Warwick CV35 ORR, U.K.

Corresponding author: Augustine Ikpehai (augustine.ikpehai@stu.mmu.ac.uk)

This work was supported in part by the Smart In-Building Micro Grid for Energy Management Project through EPSRC under Grant EP/M506758/1 and in part by the Innovate U.K. Project under Grant 101836.

ABSTRACT Power line communication (PLC) has made remarkable strides to become a key enabler of smart grid and its applications. Existing PLC systems are based on orthogonal frequency division multiplexing (OFDM), which has a high peak-to-average power ratio (PAPR). This paper presents vector OFDM (VOFDM) with advanced signal processing at the receiver to improve the energy efficiency of the PLC system. Results show that, due to its low PAPR properties, VOFDM is less sensitive to impulsive noise and provides a reduction of 5.8 dB in transmit power requirement relative to conventional OFDM. Furthermore, unlike the existing impulsive noise cancellation methods, the adopted signal processing technique also improves the SNR at the receiver by 2.1 dB, which further reduces the power requirement of the PLC transceiver. Together, these can simplify design, reduce cost, and improve energy efficiency of future PLC transceivers.

INDEX TERMS Dynamic power threshold-based estimation, energy efficiency, power-line communication (PLC), signal-to-noise ratio (SNR), smart grid, vector OFDM (VOFDM).

I. INTRODUCTION

The energy industry is in the centre of unprecedented transformation. As the smart grid evolves and the number of interconnected devices rises, energy efficiency of the enabling communication systems has become a topical issue.Although smart gridwill be supported by heterogeneous set of communications systems [1]–[5], one of the main advantages of PLC is that it reduces the cost of communication by using the existing electrical infrastructure. PLC is a technique for conveying data through the power cables traditionally used for electricity distribution. Generally, PLC systems can be grouped in terms of frequency of operation into narrowband (below 500 KHz) and broadband (1.8–100MHz). However, given that the power cables were not custom-made for communication, they pose severe challenges to data signals. The challenges include frequency selectivity, varying impedance, limited transmit power, multi-pathing, attenuation and non-Gaussian noise [6]. Noise in power line can be grouped into coloured background noise and impulsive noise, with the latter being dominant. These factors degrade system performance in terms of achievable data rate, latency and signal-to-noise ratio (SNR) at the receiver [4].

The power amplifier is one of the main energy-consuming components of the transmitters [7], [8]. To achieve maximum power efficiency, the power amplifiers operate in the dynamic range [9]. Energy efficiency and spectral efficiency are two important characteristics of the power amplifier. While spectral efficiency provides the data rate needed by smart grid applications, energy efficiency ensures that optimum number of bits per unit energy is transmitted. Therefore, optimised design of power amplifiers is crucial to the energy efficiency of PLC systems. PLC transceivers consume power in two forms; static and dynamic power. While the the static power is fixed [10], the dynamic power (transmit power) depends on the traffic load. Thus, the energy efficiency challenge can be approached from different perspectives including circuit design as well as signal processing [11].

PLC standards for smart grid applications such as power-line intelligent metering evolution (PRIME), G3-PLC, IEEE 1901.2 and Homeplug Green PHY are based on OFDM. However, the main drawback of OFDM is its high peak-to-average power ratio (PAPR) [12], [13] which reduces the energy efficiency of PLC transmitters. Solving the high PAPR problem requires highly linear power amplifiers which are

impracticable because of their high cost and large size. Hence, non-linear power amplifiers are mostly deployed.

Although many studies have reported the low PAPR of vector-OFDM (VOFDM) [14]–[19], they mostly focused on wireless systems. Recently, [20] and [21] investigated VOFDM for non-Gaussian channels, including power lines. The studies found that VOFDM generally provides better performance than OFDM in PLC. In particular, [20] showed that VOFDM exhibits lower PAPR than conventional OFDM. The benefits of low PAPR in PLC systems design include the use of inexpensive, non-linear power amplifiers as well as energy-efficient transmission. Therefore, energy efficiency is a key consideration in the development of future PLC systems.

This paper exploits the lower PAPR property of VOFDM for more efficient cancellation of impulsive noise at the receiver in order to improve the energy efficiency of PLC systems. In conventional impulsive noise cancellation techniques such as blanking, received signals are nulled when their power exceeds a predefined blanking threshold (T_b). The challenge with this approach is that detailed noise characteristics, such as signal-to-impulsive-noise ratio (SINR) and the probability of occurrence p, must be known apriori at the receiver in order to accurately determine the optimal value of T_b to be used [22]. Hence, suboptimal threshold values and short-term changes in impulsive noise characteristics can degrade performance. To address this issue in VOFDM, this paper employs the dynamic peak-based threshold estimation (DPTE) technique and refers to the new system as VOFDM-DPTE. DPTE relies on the premise that if VOFDM symbol peaks measured at the transmitter are correctly received by the blanker, output SNR can be significantly improved without regard to the short term variation in impulsive noise characteristics, a major weakness of conventional optimal blanking (COB) [23]. In reality, VOFDM symbol peak values could be sent as control information through dedicated channels or contention-free time slots. Therefore, the idea of combining VOFDM with DPTE in this paper is that together, they can significantly improve energy efficiency of the PLC systems.

The contribution of this paper is two-fold. First, we determine the dependence of symbol peaks on number of vector block (VBs) in VOFDM systems and the potential impact of the former on transmit power requirement of the power amplifier. The second contribution is the improvement of blanker output SNR using the DPTE technique. Results show that the proposed VOFDM-DPTE method significantly reduces transmit power and improves SNR at the receiver. The VOFDM-DPTE method can simplify design, reduce cost, improve energy efficiency and electromagnetic conformance of PLC transceivers.

The rest of the paper is organised as follows. In Section II, previous work in energy improvement techniques in PLC is reviewed. The system model and the effects of communication networks on smart grid applications are discussed in Sections III and IV, respectively. Section V presents the DPTE technique in VOFDM while Section VI examines the relationship between signal peaks and transmit power. Section VII analyses the performance of the proposed VOFDM-DPTE technique while Section VIII concludes the paper with highlights of its main results.

II. RELATED WORK

Compared with other aspects, little work has so far been done on energy efficiency of PLC systems. Energy efficiency in PLC can be studied with practical and information theoretic approaches [11]. Early work in this area includes [24] which employed distributed space-time block codes to reduce transmit power requirement in multi-hop PLC networks. Subsequently, [25] investigated power saving using opportunistic decoding in a decode-and-forward (DF) cooperative relaying network while [11] considered energy efficiency as resource allocation problem where the amount of information to be transmitted is the objective and energy is the resource to be minimised. Recently, different aspects of relaying have been investigated with a view to improving energy efficiency of PLC systems [26], [27]. For example, [26] and [28] considered energy harvesting at the relay nodes in a cooperative PLC network. Both studies concluded that energy efficiency can be remarkably improved if PLC nodes are capable of harvesting the unwanted high energy of non-Gaussian noise in the power line channel.

In terms of experimental studies, [29] reported that in a DF relay-assisted PLC network, energy efficiency can be improved by optimal time allocation in the relaying scheme. In the same experiment (with typical commercial modems), it was also found that power consumption consists of static and dynamic (transmit power) components, while the static power is fixed, the transmit power is load-dependent. A recent measurement campaign across six European countries [30], concluded that static power consumption in PLC networks can be reduced by deploying DF multiple-input, multiple-output (MIMO) relays. Further experiments with the MIMO PLC devices [31] revealed that although energy consumption is mostly dominated by static power, dynamic power can be up to about 50% in some modems, with the average being 40%. Within the dynamic power, it was observed that reception consumes less energy than transmission by 20-25%. These works were based on conventional OFDM and from the energy consumption pattern described above, high PAPR of OFDM will be more challenging in the uplink[1] in resource-constrained devices such as smart meters [32]. These are indications that significant energy savings can be achieved by optimising transmitter design in future PLC systems.

To reduce PAPR in OFDM systems, different techniques have been proposed, such as amplitude clipping, tone reservation, partial transmit sequence [33] and selective mapping [13], [34]. However, such techniques may cause signal distortion. On the other hand, various aspects of VOFDM have been studied in wireless systems [18], [35], [36], [37], [14].

[1] Uplink represents transmissions from the homes to utility

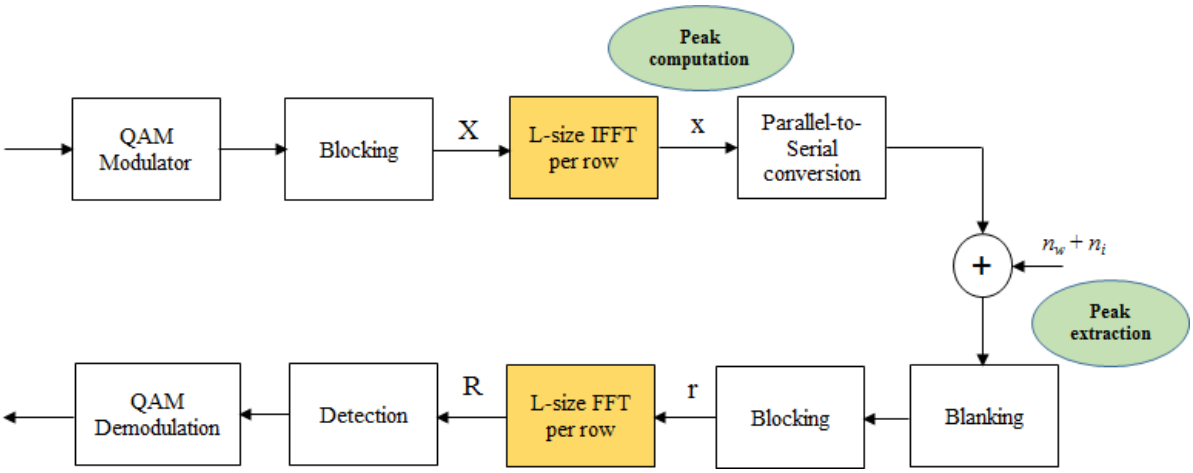

FIGURE 1. VOFDM-DPTE system diagram with the peak extractor at the receiver.

Among other outcomes, these studies found and agreed that in frequency-selective channels, VOFDM generally improves system performance [18] relative to OFDM and that the gain increases with the number of VBs. Specifically, studies such as [15]–[19] showed that VOFDM exhibits lower PAPR than conventional OFDM systems. However, to the best of our knowledge, only [20] and [21] have so far investigated VOFDM over power lines.

Furthermore, impulsive noise has been identified as a major performance inhibitor in PLC [4], [23], [38]. To mitigate the harmful effects of impulsive noise on communication signals, a number of techniques have been proposed. The simplest and most common approach is to precede the OFDM demodulator with a memory-less, non-linear preprocessors such as a blanker or clipper [39]–[42]. In line with that, [20] employed conventional blanking and clipping techniques in VOFDM-based PLC systems. The main drawback of these conventional methods is that, in order to accurately determine the thresholds, impulsive noise characteristics must be known apriori through detailed measurements. During such measurements, transient variations in the impulsive noise characteristics may be undetected. Therefore, this method is prone to blanking errors arising from sub-optimal threshold values and transient variations in impulsive noise characteristics both of which degrade performance severely [23] and can be costly in critical networks such as smart grid.

However, it has been found that DPTE provides the upper bound of blanking in OFDM systems [23], [43]. The principle of DPTE is that if the peak of every VOFDM symbol can be accurately determined and correctly received by the blanker, impulsive noise can be mitigated without apriori knowledge of its characteristics. Although the DPTE in OFDM was later enhanced in [44] where partial transmit sequence (PTS) was applied at the transmitter, the additional gain in the output SNR was at the expense significantly high computational complexity due to several optimisation iterations. Hence, this method is not attractive for resource-constrained devices. Rather, this paper, exploits the inherently low PAPR feature of VOFDM and high receiver SNR gain of DPTE to improve the energy efficiency of PLC transceivers independent of changes in impulsive noise characteristics. The detailed description of DPTE in VOFDM is given in Sec. V.

III. SYSTEM MODEL

The VOFDM system model considered in this work is illustrated in Fig.1 in which the modulated symbols are processed block by block.

VOFDM is a generalization of the conventional OFDM approach. This figure shows the transmitter and receiver sides of the VOFDM system. At the transmitter, the information bits are first mapped using the quadrature amplitude modulation (QAM) modulation to produce base-band QAM symbols denoted as X. Then a sequence $\{x_n\}_{n=0}^{N-1}$ of N modulated symbols is column-wise blocked to L vectors each of length M, i.e. $N = ML$. These vectors will be referred to as VBs. Accordingly, the l^{th} VB can be represented as

$$\mathbf{x}_l = [x_{lM},\, x_{lM+1}, \ldots x_{lM+M-1}]^T \quad l = 0, 1, \ldots, L-1 \tag{1}$$

The transmit VB, $\mathbf{x}_l$ is reshaped into a matrix of M rows and L columns such that $N = LM$. VOFDM then performs L size inverse fast Fourier transform (IFFT) over the L VBs component-wise as illustrated in Fig. 1. The VOFDM time domain signal after the IFFT can be expressed as

$$\bar{\mathbf{x}}_q = \frac{1}{\sqrt{L}} \sum_{l=0}^{L-1} \mathbf{x}_l \exp\left(\frac{j2\pi ql}{L}\right), \quad q = 0, 1, \ldots, L-1 \tag{2}$$

which can also be expressed in a vector form as

$$\bar{\mathbf{x}}_q = \left[\bar{x}_{qM}, \bar{x}_{qM+1}, \ldots, \bar{x}_{qM+M-1}\right]^T \quad q = 0, 1, \ldots, L-1. \tag{3}$$

Similar to conventional OFDM, the vectors $\{\bar{\mathbf{x}}_q\}_{q=0}^{L-1}$ in (3) are reshaped to a length N vector

$$\left[\bar{\mathbf{x}}_0^T,\ \bar{\mathbf{x}}_1^T, \ldots, \bar{\mathbf{x}}_{L-1}^T\right] = [\bar{x}_0, \bar{x}_1, \ldots, \bar{x}_{N-1}]. \tag{4}$$

Accordingly, the PAPR of this signal is

$$\text{PAPR} = \frac{\max\left(|\bar{x}_k|^2\right)}{\mathbb{E}\left[|\bar{x}_k|^2\right]}, \quad k = 0, 1, \ldots, N-1 \tag{5}$$

where max(.) is the maximum argument, |.| is the absolute value and $\mathbb{E}[.]$ denotes the expectation operator. The VOFDM signal is transmitted over the PLC channel where it is corrupted by the background and impulsive noise. In the time-domain (with perfect synchronisation assumed), the q^{th} received VOFDM symbol vector and the q^{th} received VB can be respectively expressed as

$$\bar{\mathbf{r}} = [\bar{r}_0,\ \bar{r}_1,\ \ldots,\ \bar{r}_{N-1}]^T \tag{6}$$

$$\bar{\mathbf{r}}_q = \left[\bar{r}_{qM},\ \bar{r}_{qM+1},\ \ldots,\ \bar{r}_{qM+M-1}\right]^T \tag{7}$$

Without loss of generality, it is also assumed that the signal variance is normalised to unity such that $\sigma_s^2 = (1/2)\,\mathbb{E}[|x_k|^2] = 1$, $\sigma_w^2 = (1/2)\,\mathbb{E}[|n_w|^2]$ and $\sigma_i^2 = (1/2)\,\mathbb{E}[|n_i|^2]$. This paper applies the Bernoulli-Gaussian (BG) model for generating impulsive noise such that [45]

$$i_k = \mathfrak{b}\, g_k, \quad k = 0, 1, 2, \ldots, N-1 \tag{8}$$

where g_k is complex white Gaussian noise with mean zero and $\mathfrak{b}$ is the Bernoulli process with probability $\Pr(\mathfrak{b} = 1) = p$. Therefore, the probability density function (PDF) of the total noise $n_t = n_w + n_i$, is given by

$$\begin{aligned} P_{n_t}(n_t) &= \sum_{[m=0]}^{1} p_m \mathcal{G}\left(n_t, 0, \sigma_m^2\right) \\ &= p_0 \mathcal{G}\left(n_t, 0, \sigma_0^2\right) + p_1 \mathcal{G}\left(n_t, 0, \sigma_1^2\right) \end{aligned} \tag{9}$$

where n_w and n_i are the background and impulsive noise components, respectively. It should be noted that $\bar{x}_k$, n_w and n_i are assumed to be mutually independent and the noise is uncorrelated with the data signal suchthat $\mathbb{E}\left[n_w \bar{x}_k^*\right] = \mathbb{E}\left[n_i \bar{x}_k^*\right] = 0$. $\mathcal{G}(.)$ is the Gaussian PDF given as $\mathcal{G}\left(x, \mu, \sigma_x^2\right) = \frac{1}{\sqrt{2\pi\sigma_x^2}} \exp\left(-\frac{(x-\mu)^2}{2\sigma_x^2}\right)$, $p_0 = (1-p)$, $p_1 = p$, $\sigma_0^2 = \sigma_w^2$ and $\sigma_1^2 = \sigma_w^2 + \sigma_i^2$. The variances σ_w^2 and σ_i^2 denote the background and impulsive noise powers from which the input SNR and SINR can be respectively computed as $\text{SNR} = 10\log_{10}\left(\frac{\sigma_s^2}{\sigma_w^2}\right)$ and $\text{SINR} = 10\log_{10}\left(\frac{\sigma_s^2}{\sigma_i^2}\right)$, where σ_s^2 is the transmitted signal variance.

At the receiver, in order to suppress impulsive noise, the blanker is situated before the OFDM demodulator. For each received symbol, the side information is QAM-demodulated, from which the peak estimator extracts the peak value corresponding to the VOFDM symbol and adjusts the threshold of the blanker accordingly. The received signal $\bar{r}_k$ is then passed through the blanker where it is nulled when it exceeds a certain threshold defined according to the associated peak value. That way, the blanking process adapts to changes in the peak value and determines the blanking threshold independent of the impulsive noise characteristics. In principle, the COB is described as

$$y_k = \begin{cases} \bar{r}_k, & |\bar{r}_k| \le T_b \\ 0, & |\bar{r}_k| > T_b \end{cases} \quad k = 0, 1, \ldots, N-1 \tag{10}$$

where y_k is the output of the nonlinear preprocessor and T_b is the blanking threshold. It is worth noting that careful selection of T_b is important to ensure optimal performance of the blanking device. Hence, non-linearity (10) reduces the effect of large received signal values as they are assumed to result from impulsive noise.

Next, we column-wise block $\{y_0, y_1, \ldots, y_{N-1}\}$ to an $M \times L$ matrix and then perform the fast Fourier transform (FFT) over every row to produce the frequency domain signal. This matrix is then reshaped to produce a $1 \times N$-size vector before performing the base-band demodulation and decision. Instead of just COB, DPTE is employed and the performance of the two systems are compared.

IV. EFFECTS OF COMMUNICATION NETWORK ON SMART GRID APPLICATIONS

To illustrate how services within smart grid could be impacted by the PLC network, this section presents the effects of network variability on smart grid applications performance. The underlying communication system in smart grid must seamlessly support automation, sensing and control through a bi-directional exchange of information- this is the promise of smart grid. The PRIME standard defines the physical layer (PHY) and media access control (MAC) specifications for narrowband PLC (NPLC). The PHY features include OFDM (combined with long cyclic prefix of $192\mu s$) to provide delay spread used to combat frequency selectivity while the MAC includes automatic repeat request (ARQ), TDMA over CSMA/CA (for contention-free transmission) and DPSK modulation schemes. PRIME supports DBPSK, DQPSK and D8PSK.

Although literature abound in this area, they mostly describe system performance at the PHY in terms of bit error rate (BER) results of the underlying power line channel [46]. In order to maximise the potentials of PLC, it is necessary to assess the smart grid as an integrated system. The simulation in this section is based on PRIME v1.4 standard and includes not only realities such as effects of impulsive noise but also accounts for key network performance metrics such as latency and throughput in smart grid networks using NS-3 tool. It should be noted that the use of PLC in smart grid is not restricted to NPLC, in practice there are smart meters embedded with BPLC chips and other BPLC-enabled smart grid applications.

Fig. 2 illustrates variation of the network performance with application data sizes between a smart meter and a data concentrator (DC) in the low voltage domain. The figure

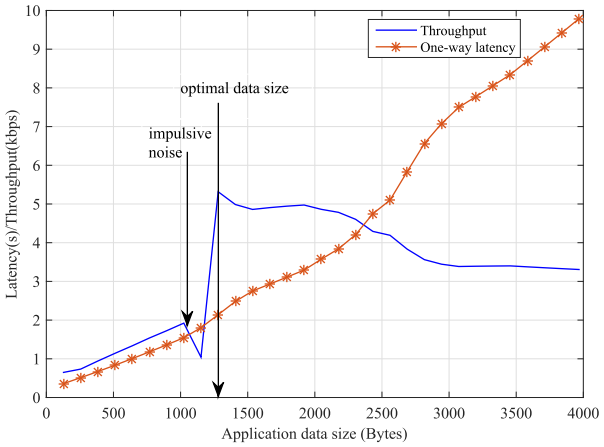

FIGURE 2. Variation of communication delay with throughput and data size using uncoded OFDM with DBPSK.

shows that there exists an optimal data size at which the PLC network maximises delivery of packets from smart meters to the DC. However, the first notch observed in the figure can be attributed to transient network impairment due to impulsive noise. This is a classic example of the effect of impulsive noise on data signal which can be explained as follows. The interference arising from the impulsive noise events creates a domino effect in which SINR reduces, followed by PHY data rate reduction. Reduced PHY data rate forces packets to remain in the transit for longer period during which they could be corrupted, damaged or lost. In fact, this effect is worse in sensitive applications such as smart metering that depend on reliable transport protocols such as transmission control protocol (TCP). For such applications, packet retransmission implies that, successful packets will remain in the buffer until all packets belonging to the same fragment or flow are received before they are passed to the application layer. Although this improves reliability, it does so at the expense of increased latency, higher computational overhead and lower goodput (useful throughput at application layer). From the result in Fig. 2, although the network recovered after the impulsive noise activity, such sporadic events can severely degrade smart grid application performance. Therefore, to provide acceptable quality of service to smart grid applications, effective techniques must be developed to mitigate the harmful effects of impulsive noise on data signals.

V. DYNAMIC PEAK-BASED THRESHOLD ESTIMATION TECHNIQUE IN VOFDM

This section describes the DPTE technique and its application for impulsive noise cancellation at the receiver. As mentioned in Sec. II, the main challenges of COB are that it requires detailed measurements of impulsive noise characteristics at the receiver and does not sufficiently account for short-term variations in impulsive noise characteristics. The optimal blanking threshold in the conventional VOFDM system is determined based on the impulsive noise parameters whereas in the proposed VOFDM-DPTE system, the optimal threshold is obtained by simply using the VOFDM symbol peak values. Instead, DPTE measures symbol peaks at the transmitter and sends the values to the blanker. If the peak estimates are correctly received, blanking can be performed even without the knowledge of the impulsive noise characteristics by the receiver. In this paper, using n symbols and N subcarriers which can be reshaped into $N = M \times L$, information bits are generated, mapped and blocked into VBs as described in Sec. III. The corresponding VOFDM symbol $\{x^{(k)}\}$ is then generated and its peak value $Peak(k)$ is determined. Thereafter, $\{x^{(k)}\}$ is transmitted through the PLC channel where it is contaminated with noise vector $\{n^{(k)}\}$ (a composition of background and impulsive noise) to produce received signal $\{r^{(k)}\}$. $\{x^{(k)}\}$, $\{n^{(k)}\}$ and $\{r^{(k)}\}$ are vectors such that $k = 0, 1, 2, ..., n$.

In practical systems, $Peak(k)$ can be sent as side information to the receiver as part of control messages through dedicated channels or contention-free timeslots such as TDMA slots defined in IEEE 1901.1, PRIME v1.4 and other NPLC standards for smart grid. At the receiver, the peak estimator extracts the $Peak(k)$ value associated with the k^{th} symbol and dynamically adjusts the blanking threshold accordingly. The k^{th} VOFDM symbol is subjected to blanking operation according to $Peak(k)$. The process is then repeated with COB and compared with DPTE in terms of output SNR. It was shown in [23] that the optimal blanking threshold varies linearly with OFDM symbol peak values. This relationship also exists in VOFDM systems, being a generalised form of OFDM; however, this work exploits the relatively lower symbol peak in VOFDM to simplify impulsive noise detection and cancellation at the receiver.

VI. SIGNAL PEAKS AND TRANSMIT POWER IN VOFDM

The total power consumed, P_T, by a PLC transceiver is a combination of static and dynamic power. This can be expressed as [29]

$$P_T = P_0 + P(l) \tag{11}$$

where l is the transmitted traffic load in bits/s or packets/s. P_0 is the power consumed (in Watts) in idle state and is fixed for a given device while $P(l)$ is an increasing function of load (dynamic power). The inevitable choice of OFDM in current PLC systems is at the expense of high PAPR. High PAPR requires highly-linear power amplifier at the transmitter which are bulky, complex and expensive. In the absence of that, high PAPR can cause the power amplifier to be overloaded after which it transits to nonlinear operation (distortion). This phenomenon results in low power efficiency [47], [48] and unwanted electromagnetic emissions [49], [50]. The low power efficiency results in higher amount of energy wasted through heat dissipation [8].

For a conventional OFDM transmitter, P_T represents the sum of the power consumed by the linear power amplifier and the one consumed by other circuit blocks, P_C, (usually very small). In practical systems, energy efficiency of the power

amplifier is typically low, for example it is 20-35% in wireless systems [7]. Considering that smart grid will interconnect several millions of devices, energy-efficient communication systems is a key factor in its design. In addition to applications peculiarities, energy efficiency depends on variables such as hardware components, the power consumption of the power amplifier, load characteristics and operating frequency [7]. For example, let us consider the Class-A power amplifiers which are the most linear. They consume a constant P_{DC} regardless of the input power [47]. The power amplifier's energy efficiency is defined as the portion of P_{DC} delivered to the load and can be expressed as

$$\eta_{EE} = \frac{P_{out,ave}}{P_{DC}} \tag{12}$$

where $P_{out,ave}$ is the average output power of the power amplifier, P_{DC} is the DC power consumed by the power amplifier and $P_{DC} >> P_C$. Under a perfect linear condition, the energy efficiency approximates to [47]

$$\eta_{EE} = \frac{0.5}{PAPR}. \tag{13}$$

Clearly, a reduction of PAPR will result in higher energy efficiency of the power amplifier, hence, timely techniques are needed to reduce PAPR in PLC systems.

As presented in Sec. III, VOFDM uses relatively smaller IFFT size than conventional OFDM. However, since it is practically challenging in multi-carrier systems to accurately determine the peak of every VOFDM symbol, it is common to apply complimentary cumulative distribution function (CCDF) in such estimations. Therefore, this work adopts the CCDF expression (14), which is widely used in the literature. Here, the CCDF is defined as the probability that the peak of VOFDM symbols exceeds a certain value $Peak_0$ and can be written as

$$\text{CCDF} = 1 - \Pr\{\text{Peak} \leq \text{Peak}_o\} = \Pr\{\text{Peak} > \text{Peak}_o\}. \tag{14}$$

Although (14) is not precise for every symbol, it was shown in [23] that such approximation adequately represents average system performance. It is now necessary to establish the effects of the number of VBs on CCDF of VOFDM symbol peaks compared with typical OFDM. Based on (14), we conducted extensive simulations to determine the CCDF at different peak values for various numbers of VBs. Fig. 3 depicts the variation of VOFDM symbol peak with the number of VBs, where $M = 1$ is equivalent to conventional OFDM.

Two cases: $N = 512$ and $N = 1024$ with various VBs are considered. Fig. 3 shows clearly that provided there are more than one VB, ($M > 1$), VOFDM achieves lower peak values than the typical OFDM system and that the symbol peaks reduce as the number of VBs increases. It is seen that for a given peak value $Peak_0$, CCDF decreases as the number of VBs in the VOFDM system increases. This brings new flexibilities into design of PLC systems. Furthermore, unlike the COB, shifting peak estimation to the transmitter-side relieves the receiver of some computational overhead which can further lessen the effect of transmitter-receiver unbalanced complexity in systems design. Also, for each number of VBs, the performance gap between VOFDM and OFDM closes as the number of subcarriers increases from 512 to 1024. The figure generally indicates that for a fixed N, as the number of VB increases, VOFDM symbol peaks becomes less likely to be higher than the estimate $Peak_0$. For example, in Fig. 3b, it is observed that in VOFDM, the symbol peak values are more likely to be higher than 9 dB as the number of VBs decreases from 128. It can generally also be inferred that although the symbol peak value of VOFDM decreases with the number of VBs but that comes at the expense of computational complexity. However, ultra-fast chips are readily available at reasonably low cost to ease implementation.

Finally, it is observed in Fig. 3a that by applying VOFDM ($M = 128$) to QAM modulated signal with $N = 512$, symbol peak power reduces by about 5.8 dB relative to conventional OFDM. The practical implication is that in PLC-based smart grid, if 20 dBm is required to transmit QAM symbols with OFDM, the transmitter's power amplifier needs a maximum of 31.8 dBm to ensure linear operation whereas with VOFDM, maximum of 26.1 dBm is needed. When aggregated over several thousands or millions of PLC nodes, this could yield significant power savings.

VII. OUTPUT SNR PERFORMANCE OF VOFDM-DPTE SYSTEM

A. OUTPUT SNR OF THE BLANKER

This section presents the transmit power savings achievable when VOFDM is implemented with DPTE in PLC transceivers. This is done by computing the SNR at the output of the blanking device. However, it is necessary to briefly review the blanker output SNR of COB with various blanking thresholds T_b. In that regard, we investigate the SNR performance of different VBs in VOFDM and compare the results with OFDM using the COB technique. The blanking procedure is then repeated using the proposed technique and performance between DPTE and COB is compared. To do this, we consider the SNR at the output of the non-linear preprocessor which can be computed for the VOFDM as [51]

$$SNR_1 = \frac{\mathbb{E}\left[|K_0 \bar{x}_k|^2\right]}{\mathbb{E}\left[|y_k - K_0 \bar{x}_k|^2\right]} \tag{15}$$

where K_0 is a real constant chosen as $K_0 = (1/2)\,\mathbb{E}\left[\left|y_k \bar{x}_k^*\right|^2\right]$.

For OFDM, output SNR is given by

$$SNR_2 = \frac{2K_1^2}{E_1 - 2K_1^2} \tag{16}$$

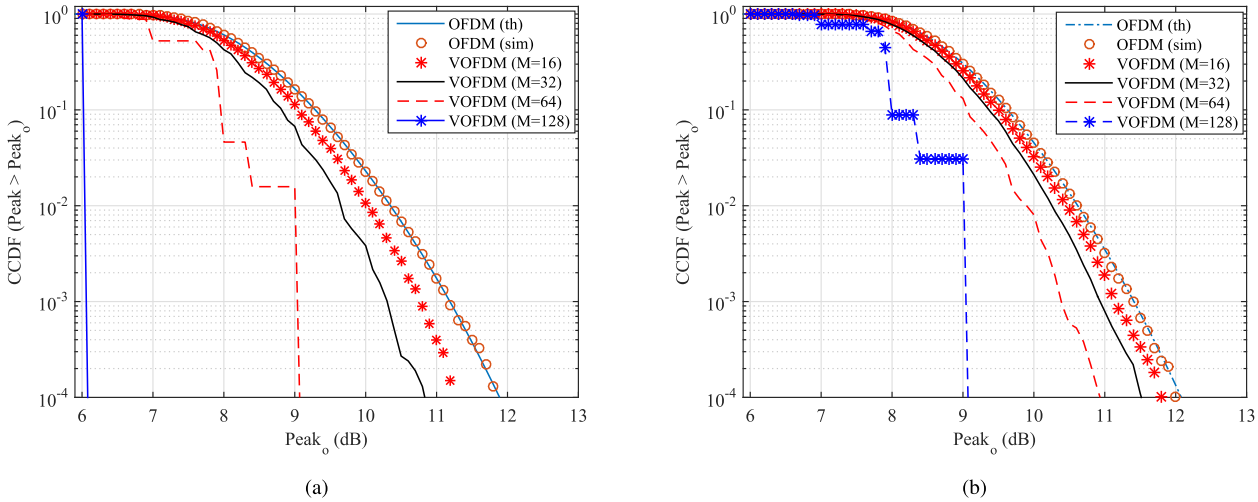

FIGURE 3. CCDF as a function of VOFDM symbol peak values for various N and VB ($M = \{16, 32, 64, 128\}$) using 10^5 symbols. Analytical and simulated CCDF of the conventional OFDM are also included. (a) CCDF of symbol peak values when $N = 512$. (b) CCDF of symbol peak values when $N = 1024$.

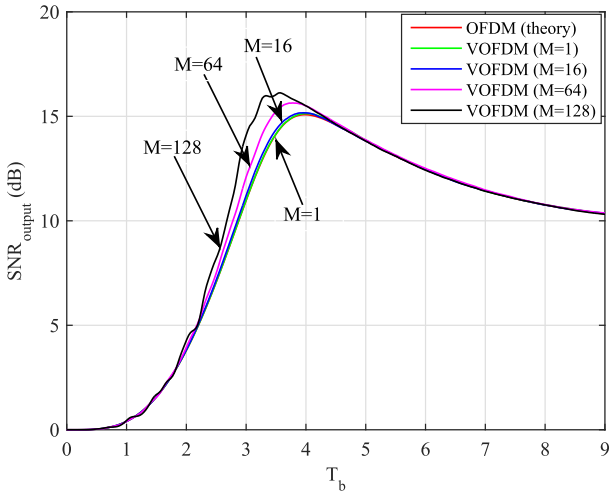

FIGURE 4. Output SNR performance of the VOFDM system versus the blanking threshold when the input SNR=25 dB, SINR=−10 dB and $p = 0.01$. $N = 512$, $n = 10^4$ and 16QAM.

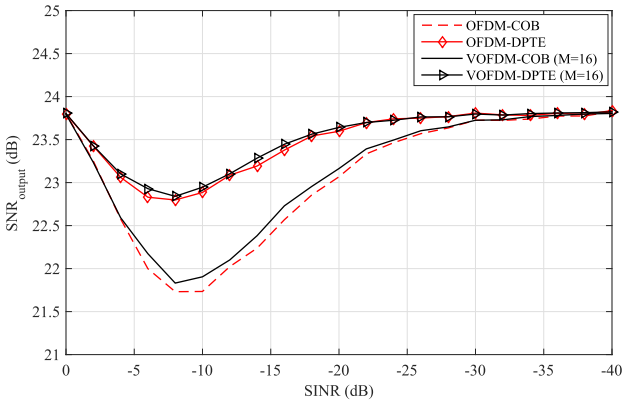

FIGURE 5. SNR performance of DPTE and COB in VOFDM system with input SNR=25 dB, $p = 0.001$, n =5*10^4 and $N = 256$.

where

$$K_1 = 1 - \sum_{i=0}^{L-1} p_i \left[\exp\left(-\frac{T_b^2}{2\left(1+\sigma_i^2\right)} \right) + T_b\, \Xi \right] \quad (17)$$

$$E_1 = 2 + 2\sum_{i=0}^{L-1} p_i \left(\sigma_i^2 - \Gamma \right) \exp\left(-\frac{T_b^2}{2\left(1+\sigma_i^2\right)} \right) \quad (18)$$

where E_1 is the total signal power at the output of the nonlinear preprocessor, $\Xi = \frac{T_b}{2(1+\sigma_i^2)} \exp\left(-\frac{T_b^2}{2(1+\sigma_i^2)} \right)$ and $\Gamma = 1+T_b^2+\sigma_i^2$ [51]. The noise parameters used in this evaluation are input SNR = 25 dB, SINR = −10 dB and $p = 0.01$.

Simulation results of OFDM and VOFDM are obtained using (15). Fig. 4 illustrates the achieveable SNR at the output of the blanker using the COB method. First, it is observed that analytical result agrees with the simulation. Within the intermediate region, this figure shows that VOFDM ($M = 128$) achieves a maximum of about 2 dB SNR improvement over conventional OFDM. The figure also reveals that for all $M > 1$, VOFDM always outperforms OFDM. However, when the T_b is too low, the SNR degrades rapidly as part of data signal power is lost during blanking. Conversely, when T_b is too high, some of the impulsive noise samples push through the system undetected, thereby degrading the SNR at the receiver. It is further observed at these extreme blanking thresholds that OFDM achieves the same performance as VOFDM. Between these extremes, there exists a value of T_b which maximises the output SNR of the blanker. Next, we compare the SNR performance of DPTE and conventional blanking techniques.

Fig. 5 compares the output SNR performance between DPTE and COB in OFDM and VOFDM. It is clear that DPTE outperforms COB. This result demonstrates that if a

certain QAM modulated symbol sequence of length N signal is blanked using the DPTE technique, even with OFDM and 16 VBs, the output SNR can be improved by 1.1 dB in each case relative to COB. The figure further shows that at extreme values (very low and very high) of SINRs, the output SNR is not affected by the number of VBs in VOFDM, as it becomes identical for both systems. This is logical because at one extreme, when SINR is very high, the system tends to behave as if impulsive noise does not exist, yielding maximum SNR. Given that amplitude of the affected symbols is typically higher than the average amplitude of symbols, at the other extreme, when SINR is very low, impulsive noise samples can be more easily detected and cancelled which also results in maximum SNR. Following from Fig. 5, the output SNR is expected to improve as the number of VBs increases. That is presented and analysed in the remaining part of this section.

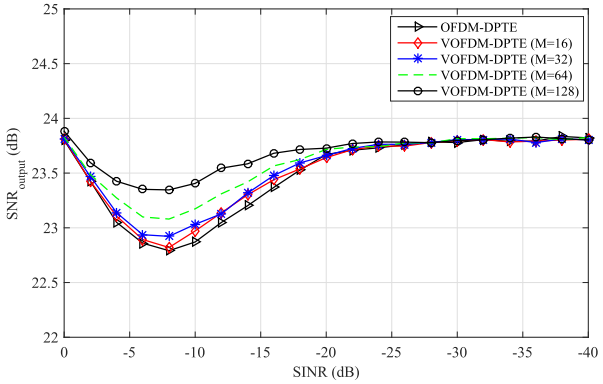

FIGURE 6. Blanker output SNR as a function of SINR of the VOFDM-DPTE with parameters $N = 256$, $n = 10^4$ symbols in 16QAM, $p = 0.001$ and the input SNR = 25 dB.

Fig. 6 presents the variation of the output SNR with SINR for different numbers of VBs. It is obvious from the results that the output SNR performance improves with the number of VBs. This result underscores the earlier observation in Fig. 5. For example, at M=128, DPTE can increase the output SNR by about 0.6 dB compared with the case when M=16.

B. COMPARATIVE SNR PERFORMANCE FOR VARIOUS IMPULSIVE NOISE CASES

In a smart grid where several thousands or millions of heterogeneous devices with different operational characteristics are interconnected, the probability of impulsive noise can be significantly high. Here we investigate the SNR performance of DPTE and COB in different impulsive noise conditions.

Fig. 7 compares the output SNR of DPTE with COB in a VOFDM system under various channel conditions based on impulsive noise events. It is observed that for all VBs, DPTE consistently outperforms COB. It can also be seen that the output SNR improves with the number of VBs such that the peak SNR is achieved when M=128, yielding a maximum SNR improvement of about 2.1 dB over COB. Finally, the figure reveals that at extreme SINRs, the output

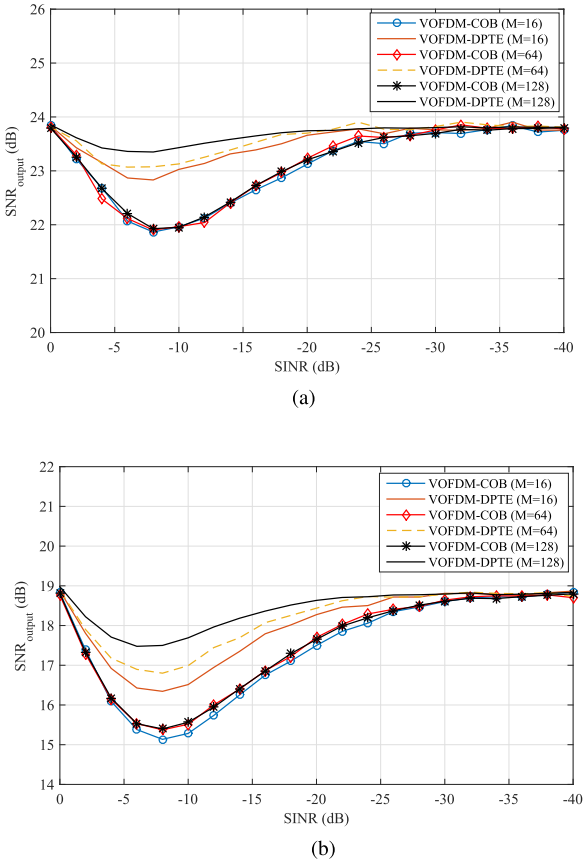

FIGURE 7. Comparative SNR performance of DPTE and COB in various impulsive noise conditions using $p = \{0.001, 0.01\}$, SNR=25, $N = 256$, 16QAM and $n = 10^4$. (a) when $p = 0.001$. (b) when $p = 0.01$.

SNR is independent of the number of VBs. The functional consequence of these results is that unlike OFDM ($M = 1$), the existence of M= {16, 32, 64, 128...} in VOFDM provides significant flexibility in system design as complexity can now be matched with performance without loosing the fundamental benefits of OFDM as a multi-carrier system.

C. DPTE GAIN RELATIVE TO COVENTIONAL BLANKING

This section presents the SNR gain of DPTE technique relative to COB for different probabilities of impulsive noise. The relative gain $G_{Relative}$ is therefore defined as

$$G_{Relative} = 10\log_{10}\left(\frac{SNR_{DPTE}}{SNR_{COB}}\right). \quad (19)$$

The result is illustrated in Fig.8. It is clear that, given the same channel conditions, DPTE always achieves higher output SNR relative to COB. It is also observed that, the relative SNR gain increases as p decreases. For example, at $p = 0.001$ a relative gain of 2 dB is achieved, but when p increases to 0.05, the maximum gain reduces to about 0.74 dB. In both cases of $N = 256$ and $N = 512$, it is obvious that, for all values of p, there is a certain value of SINR at which $G_{Relative}$ is highest, in this figure, that value is -10dB. Finally, the mere fact that $G_{Relative} > 0$ in all cases clearly indicates

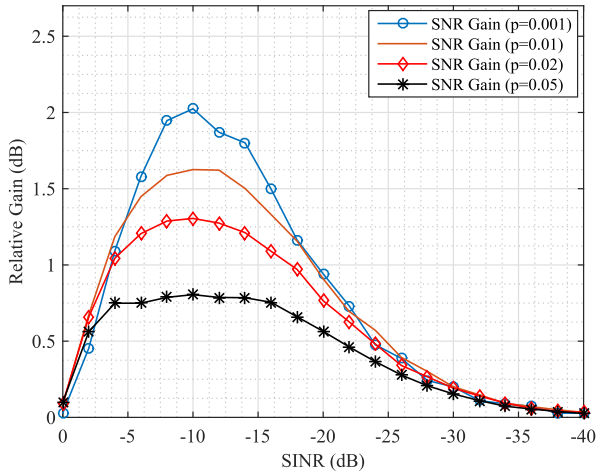

FIGURE 8. Relative SNR gain of VOFDM-DPTE over COB for different impulsive noise probabilities for $N = 256$ and $M = 64$ at input SNR=30 dB, $p = 0.05$, $n = 10^4$ and 16QAM.

that DPTE always performs better than COB, even when the peak estimates are corrupted by impulsive noise. This can be explained by the fact that DPTE dynamically tunes the blanking threshold, in the event that the side information is corrupted by impulsive noise, only a very small fraction of the peak values are affected whereas short-term variations in impulsive noise behavior may consistently be undetected in COB. Hence, given the same transmit power on both systems, DPTE is more energy efficient.

VIII. CONCLUSION

Energy-efficient communication is crucial in smart grid. However, the high PAPR in conventional OFDM affects the energy efficiency and cost of PLC systems which is more pronounced in smart grid due to its scale. To improve energy efficiency in PLC systems, this paper has shown that existence of VBs in VOFDM offers variable IFFT size which introduces new design choices to match complexity with energy efficiency. Furthermore, impulsive noise is one of the dominant challenges in PLC systems and COB is the simplest and widely used method for its cancellation. To suppress impulsive noise at the receiver, DPTE has been applied in this work. By exploiting the low PAPR and high SNR properties of VOFDM and DPTE respectively, this paper demonstrated that transmit power can be reduced by about 5.8 dB while the output SNR of the blanker is increased by 2.1 dB relative to conventional OFDM. When aggregated over several thousands or millions of nodes in a neighbourhood area network for example, this can yield massive savings in power requirements. It was observed that VOFDM performance gains came at the expense of computational complexity, however, ultra-fast, inexpensive chips are readily available to ease implementation. Hence, this is a reasonable sacrifice.

REFERENCES

[1] H. Farhangi, "The path of the smart grid," *IEEE Power Energy Mag.*, vol. 8, no. 1, pp. 18–28, Jan./Feb. 2010.

[2] S. Mudriievskyi, I. Tsokalo, A. Haidine, B. Adebisi, and R. Lehnert, "Performance evaluation of MAC backoff algorithm in narrowband PLC," in *Proc. IEEE Int. Conf. Smart Grid Commun. (SmartGridComm)*, Oct. 2011, pp. 108–113.

[3] S. Galli, A. Scaglione, and Z. Wang, "For the grid and through the grid: The role of power line communications in the smart grid," *Proc. IEEE*, vol. 99, no. 6, pp. 998–1027, Jun. 2011.

[4] A. Ikpehai, B. Adebisi, K. M. Rabie, R. Haggar, and M. Baker, "Experimental study of 6LoPLC for home energy management systems," *MDPI Energies*, vol. 9, no. 12, p. 1046, 2016.

[5] A. Ikpehai, B. Adebisi, and K. M. Rabie, "Broadband PLC for clustered advanced metering infrastructure (AMI) architecture," *Energies*, vol. 9, no. 7, p. 569, 2016.

[6] M. Rozman, A. Ikpehai, B. Adebisi, and K. M. Rabie, "Channel characterisation of cooperative relaying power line communication systems," in *Proc. IEEE Int. Symp. Commun. Syst., Netw. Digit. Signal Process.*, Jul. 2016, pp. 1–5.

[7] J. Joung, C. K. Ho, K. Adachi, and S. Sun, "A survey on power-amplifier-centric techniques for spectrum- and energy-efficient wireless communications," *IEEE Commun. Surveys Tuts.*, vol. 17, no. 1, pp. 315–333, 1st Quart., 2015.

[8] H. Ochiai, "An analysis of band-limited communication systems from amplifier efficiency and distortion perspective," *IEEE Trans. Commun.*, vol. 61, no. 4, pp. 1460–1472, Feb. 2013.

[9] L. Guan and A. Zhu, "Green communications: Digital predistortion for wideband RF power amplifiers," *IEEE Microw. Mag.*, vol. 15, no. 7, pp. 84–99, Nov. 2014.

[10] W. Bakkali, P. Pagani, and T. Chonavel, "Energy efficiency performance of relay-assisted power-line communication networks," in *Proc. IEEE Consum. Commun. Netw. Conf.*, Jan. 2015, pp. 525–530.

[11] J.-Y. Baudais, A. M. Tonello, and A. Hamini, "Energy efficient resource allocation for quantity of information delivery in parallel channels," *Trans. Emerg. Telecommun. Technol.*, vol. 27, no. 7, pp. 910–922, 2014.

[12] K. M. Rabie, E. Alsusa, A. D. Familua, and L. Cheng, "Constant envelope OFDM transmission over impulsive noise power-line communication channels," in *Proc. IEEE Int. Symp. Power Lines Commun. (ISPLC)*, Mar. 2015, pp. 13–18.

[13] J. S. Lee, H.-M. Oh, J.-T. Kim, and J. Y. Kim, "Performance of scaled SLM for PAPR reduction of OFDM signal in PLC channels," in *Proc. IEEE Int. Symp. Power Lines Commun. (ISPLC)*, Mar./Apr. 2009, pp. 166–170.

[14] J. Han and G. Leus, "Space-time and space-frequency block coded vector OFDM modulation," *IEEE Commun. Lett.*, vol. 21, no. 1, pp. 204–207, Jan. 2017.

[15] I. Ngebani, Y. Li, X.-G. Xia, H. S. Ahmed, and M. Zhao, "Analysis of phase noise in vector OFDM systems," in *Proc. IEEE Global Commun. Conf. (GLOBECOM)*, Dec. 2013, pp. 3602–3607.

[16] W. Zhou, L. Fan, and H. Chen, "Vector orthogonal frequency division multiplexing system over fast fading channels," *IET Commun.*, vol. 8, no. 13, pp. 2322–2335, Sep. 2014.

[17] Y. Li, I. Ngebani, X. G. Xia, and A. Host-Madsen, "On performance of vector OFDM with linear receivers," *IEEE Trans. Signal Process.*, vol. 60, no. 10, pp. 5268–5280, Oct. 2012.

[18] P. Cheng, M. Tao, Y. Xiao, and W. Zhang, "V-OFDM: On performance limits over multi-path Rayleigh fading channels," *IEEE Trans. Commun.*, vol. 59, no. 7, pp. 1878–1892, Jul. 2011.

[19] I. Ngebani, Y. Li, X.-G. Xia, and M. Zhao, "EM-based phase noise estimation in vector OFDM systems using linear MMSE receivers," *IEEE Trans. Veh. Technol.*, vol. 65, no. 1, pp. 110–122, Jan. 2016.

[20] B. Adebisi, K. M. Rabie, A. Ikpehai, C. Soltanpur, and A. Wells, "Vector OFDM transmission over non-Gaussian power line communication channels," *IEEE Syst. J.*, to be published.

[21] C. Soltanpur, K. Rabie, B. Adebisi, and A. Wells, "Masreliez-equalized VOFDM in non-Gaussian channels: Power line communication systems," *IEEE Syst. J.*, to be published.

[22] K. M. Rabie and E. Alsusa, "Improving blanking/clipping based impulsive noise mitigation over powerline channels," in *Proc. IEEE 24th Int. Symp. Pers. Indoor Mobile Radio Commun.(PIMRC)*, Sep. 2013, pp. 3413–3417.

[23] E. Alsusa and K. M. Rabie, "Dynamic peak-based threshold estimation method for mitigating impulsive noise in power-line communication systems," *IEEE Trans. Power Del.*, vol. 28, no. 4, pp. 2201–2208, Oct. 2013.

[24] L. Lampe, R. Schober, and S. Yiu, "Distributed space-time coding for multihop transmission in power line communication networks," *IEEE J. Sel. Areas Commun.*, vol. 24, no. 7, pp. 1389–1400, Jul. 2006.

[25] S. D'Alessandro, A. M. Tonello, and F. Versolatto, "Power savings with opportunistic decode and forward over in-home PLC networks," in *Proc. IEEE Int. Symp. Power Line Commun. Appl. (ISPLC)*, Apr. 2011, pp. 176–181.
[26] K. M. Rabie, B. Adebisi, A. M. Tonello, and G. Nauryzbayev, "For more energy-efficient dual-hop DF relaying power-line communication systems," *IEEE Syst. J.*, to be published.
[27] K. M. Rabie and B. Adebisi, "Enhanced amplify-and-forward relaying in non-Gaussian PLC networks," *IEEE Access*, vol. 5, pp. 4087–4094, 2017.
[28] K. M. Rabie, B. Adebisi, and A. Salem, "Improving energy efficiency in dual-hop cooperative PLC relaying systems," in *Proc. IEEE Int. Symp. Power Line Commun. Appl. (ISPLC)*, Mar. 2016, pp. 196–200.
[29] W. Bakkali, M. Tlich, P. Pagani, and T. Chonavel, "A measurement-based model of energy consumption for PLC modems," in *Proc. IEEE Int. Symp. Power Line Commun. Appl. (ISPLC)*, Mar./Apr. 2014, pp. 42–46.
[30] W. Bakkali, P. Pagani, T. Chonavel, and A. M. Tonello, "Energy efficiency performance of decode and forward MIMO relay PLC systems," in *Proc. IEEE Int. Symp. Power Line Commun. Appl. (ISPLC)*, Mar. 2016, pp. 201–205.
[31] W. Bakkali, P. Pagani, and T. Chonavel, "Experimental analysis and modeling of energy consumption behaviour for MIMO PLC modems," in *Proc. IEEE Global Commun. Conf. (GLOBECOM)*, Dec. 2015, pp. 1–5.
[32] M. Dohler, T. Watteyne, T. Winter, and D. Barthel, Eds., *Routing Requirements for Urban Low-Power and Lossy Networks*, document RFC5548, IETF, 2009, accessed on Feb. 10, 2017. [Online]. Available: https://tools.ietf.org/html/rfc5548
[33] T. T. Nguyen and L. Lampe, "On partial transmit sequences for PAR reduction in OFDM systems," *IEEE Trans. Wireless Commun.*, vol. 7, no. 2, pp. 746–755, Feb. 2008.
[34] K. M. Rabie and E. Alsusa, "Efficient SLM based impulsive noise reduction in powerline OFDM communication systems," in *Proc. IEEE Global Commun. Conf. (GLOBECOM)*, Dec. 2013, pp. 2915–2920.
[35] H. Zhang, X.-G. Xia, L. J. Cimini, and P. C. Ching, "Synchronization techniques and guard-band-configuration scheme for single-antenna vector-OFDM systems," *IEEE Trans. Wireless Commun.*, vol. 4, no. 5, pp. 2454–2464, Sep. 2005.
[36] H. Zhang, X.-G. Xia, Q. Zhang, and W. Zhu, "Precoded OFDM with adaptive vector channel allocation for scalable video transmission over frequency-selective fading channels," *IEEE Trans. Mobile Comput.*, vol. 99, no. 2, pp. 132–142, Apr./Jun. 2002.
[37] H. Zhang and X.-G. Xia, "Iterative decoding and demodulation for single-antenna vector OFDM systems," *IEEE Trans. Veh. Technol.*, vol. 55, no. 4, pp. 1447–1454, Jul. 2006.
[38] B. Adebisi, S. Ali, and B. Honary, "Space-frequency and space-time-frequency M3FSK for indoor multiwire communications," *IEEE Trans. Power Del.*, vol. 24, no. 4, pp. 2361–2367, Oct. 2009.
[39] S. V. Zhidkov, "Performance analysis and optimization of OFDM receiver with blanking nonlinearity in impulsive noise environment," *IEEE Trans. Veh. Technol.*, vol. 55, no. 1, pp. 234–242, Jan. 2006.
[40] S. V. Zhidkov, "On the analysis of OFDM receiver with blanking nonlinearity in impulsive noise channels," in *Proc. Int. Symp. Intell. Signal Process. Commun. Syst.*, Nov. 2004, pp. 492–496.
[41] K. Vastola, "Threshold detection in narrow-band non-Gaussian noise," *IEEE Trans. Commun.*, vol. 32, no. 2, pp. 134–139, Feb. 1984.
[42] R. Ingram, "Performance of the locally optimum threshold receiver and several suboptimal nonlinear receivers for ELF noise," *IEEE J. Ocean. Eng.*, vol. 9, no. 3, pp. 202–208, Jul. 1984.
[43] K. M. Rabie and E. Alsusa, "Quantized peak-based impulsive noise blanking in power-line communications," *IEEE Trans. Power Del.*, vol. 29, no. 4, pp. 1630–1638, Aug. 2014.
[44] K. Rabie and E. Alsusa, "Improved DPTE technique for impulsive noise mitigation over power-line communication channels," *AEU-Int. J. Electron. Commun.*, vol. 69, no. 12, pp. 1847–1853, 2015.
[45] M. Ghosh, "Analysis of the effect of impulse noise on multicarrier and single carrier QAM systems," *IEEE Trans. Commun.*, vol. 44, no. 2, pp. 145–147, Feb. 1996.
[46] J. Matanza, S. Kiliccote, S. Alexandres, and C. Rodríguez-Morcillo, "Simulation of low-voltage narrow-band power line communication networks to propagate openADR signals," *IEEE J. Commun. Netw.*, vol. 17, no. 6, pp. 656–664, Dec. 2015.
[47] R. J. Baxley and G. T. Zhou, "Power savings analysis of peak-to-average power ratio in OFDM," *IEEE Trans. Consum. Electron.*, vol. 50, no. 3, pp. 792–798, Aug. 2004.
[48] T. Jiang, C. Li, and C. Ni, "Effect of PAPR reduction on spectrum and energy efficiencies in OFDM systems with class-A HPA over AWGN channel," *IEEE Trans. Broadcast.*, vol. 59, no. 3, pp. 513–519, Sep. 2013.
[49] B. Adebisi and B. Honary, "Comparisons of indoor PLC emissions measurement results and regulation standards," in *Proc. IEEE Int. Symp. Power Line Commun. Appl.*, Mar. 2006, pp. 319–324.
[50] B. Adebisi, J. Stott, and B. Honary, "Experimental study of the interference caused by PLC transmission on HF bands," in *Proc. 10th IET Int. Conf. Ionospheric Radio Syst. Techn. (IRST)*, 2006, pp. 326–330.
[51] S. V. Zhidkov, "Analysis and comparison of several simple impulsive noise mitigation schemes for OFDM receivers," *IEEE Trans. Commun.*, vol. 56, no. 1, pp. 5–9, Jan. 2008.

AUGUSTINE IKPEHAI (GS'14) received the B.Sc. degree in physics from the University of Ibadan, Nigeria, and the M.Sc. degree in mobile and personal radio communication engineering from Lancaster University, U.K., in 2005. He is currently pursuing the Ph.D. degree in smart grid communication from the Manchester Metropolitan University, Manchester, U.K. From 2006 to 2014, he was a Network Engineer with the IT-Engineering Department, Zenith Bank Plc, Nigeria. He has extensive industry experience in IP network design, implementation, and optimization, backed with many professional certifications in Cisco and Juniper Networks. He is currently with the Division of Electrical/Electronic Engineering, Manchester Metropolitan University. His research interests include communications systems modeling, smart home, power line communication, and energy optimization in smart grid and other cyber-physical systems. He was a recipient of the MMU Knowledge Exchange Project Award and the Outstanding Knowledge Exchange Award in 2016.

BAMIDELE ADEBISI (M'06–SM'15) received the B.S. degree in electrical engineering from Ahmadu Bello University, Zaria, Nigeria, in 1999, and the M.S. degree in advanced mobile communication engineering and the Ph.D. degree in communication systems from Lancaster University, Lancaster, U.K., in 2003 and 2009, respectively. He was a Senior Research Associate with the School of Computing and Communication, Lancaster University, from 2005 to 2012. He joined Manchester Metropolitan University, Manchester, U.K., in 2012, where he is currently a Reader in electrical and electronic engineering. He has been involving in several commercial and government projects focusing on various aspects of wireline and wireless communications. He is particularly interested in the Research and Development of communication technologies for electrical energy monitoring/management, transport, water, critical infrastructures protection, home automation, IoTs, and Cyber Physical Systems. He has several publications and a patent in the research area of data communications over power line networks and smart grid. He is a member of the IET.

KHALED MAAIUF RABIE (SM'12–M'15) received the B.Sc. degree (Hons.) from the University of Tripoli, Libya, the M.Sc. degree (Hons.) from the University of Manchester, U.K., in 2008 and 2010, respectively, and the Ph.D. degree in communication engineering in 2015. In 2011, he joined the University of Manchester, where he was a part-time Member of Staff. He is currently a Post-Doctoral Research Associate with Manchester Metropolitan University (MMU), Manchester, U.K. His research interests include the signal processing and analysis of power-line and wireless communication networks. He was the recipient of several awards, both nationally and internationally, including the Agilent Technologies' Best M.Sc. Student Award, the Manchester Doctoral College Ph.D. Scholarship, and the MMU Outstanding Knowledge Exchange Project Award of 2016. He was a recipient of the best student paper award at the IEEE International Symposium on Power Line Communications and its applications in 2015, TX, US.

MICHAEL FERNANDO received the B.S. degree in electronics and communication engineering from Madurai Kamraj University, India, in 2003, and the M.Sc. degree in optoelectronic and communication systems and the Ph.D. degree in microwave imaging from Northumbria University, U.K., in 2005 and 2012, respectively. He is currently a Principal Lecturer of electrical and electronic engineering with Manchester Metropolitan University. He is also a Chartered Engineer with the IET. He has published in many journals and conferences and delivered keynote speeches in various conferences and institutions. His current research interests include microwave holography, wireless power transfer, power line communication, medical imaging applications, concealed weapon detection, and late time response system.

ANDREW WELLS (M'17) received the M.S. degree in mobile communications and the Ph.D. degree in communications system and computer science from Lancaster University, Lancaster, U.K., in 2007 and 2010, respectively. In 2011, he joined the Advanced Electrical Research Department, Jaguar Land Rover (JLR), Warwick, U.K., where he is involved in several projects focusing on the development of future infotainment and vehicle connectivity. He joined the Electrical and Electronic Software Engineering Department, JLR, and is currently the Technical Lead for JLR's cross car-line next-generation audio platform. He is particularly interested in the research and development of communication technologies for vehicle communications, Internet of Things, autonomous vehicles, and automotive security.